Electricity-Aware Charging Design of a PV/T-Assisted Open Thermochemical Storage Unit with Exhaust Heat Recovery

Jawad Javed[1,*] and Maria Jawad[1]

[1] IU International University of Applied Sciences
* Correspondence: b.jawad4891@gmail.com

Abstract: A low-temperature thermochemical energy storage solution can transform intermittent energy into charging capacity, yet the performance of an open thermochemical salt-hydrate reactor relies on the amount of useful storage that can be achieved per electricity unit. This paper poses a concentrated engineering inquiry: what architectural design, air flow condition, and dimension of the reactor bed will result in the highest charging quality with electricity awareness in a PV/T-assisted open thermochemical energy storage reactor? An internally consistent matrix of charging case studies will cover architecture, air flow rate, reactor bed thickness, and reactor bed length. Each case will be assessed with Electricity Aware Charging Quality Index (EACQI), which measures conversion degree, storage amount, PV/T input, external electricity consumption, power assurance rate, thermoeconomic efficiency, and electricity aware productivity. Integration of PV/T-TCES-HEX achieves a top-ranking EACQI of 1.000 while reducing external electricity demand by 59.47% compared with the TCES-alone architecture. Regarding operating cases, an air flow rate of 0.025 kg s^{-1} yields the optimal balanced charging quality while 0.020–0.030 kg s^{-1} creates the robust band for operation. The reactor bed thickness of 0.04 m provides the optimal balanced bed geometry and 0.05 m still serves as the leading alternative based on the storage priority. As for reactor bed length, 0.5 m emerges as the best choice regardless of the testing priorities. It is thus demonstrated that the best charging architecture is not achieved through maximizing conversion; rather, it is attained through integration of PV/T assistance, heat recovery, and reactor bed geometry.

Keywords: thermochemical energy storage; photovoltaic-thermal collector; electricity-aware design; salt hydrate reactor; heat recovery; multi-criteria ranking

Citation: Jawad Javed, Maria Jawad. 2023. Electricity-Aware Charging Design of a PV/T-Assisted Open Thermochemical Storage Unit with Exhaust Heat Recovery. *TK Techforum Journal (ThyssenKrupp Techforum)* 2023(2): 59–69.

Received: June-03-2023
Accepted: August-27-2023
Published: September-30-2023

1. Introduction

The growing interest in thermochemical energy storage (TCES) for solar-assisted heating is justified by the ability of reversible solid-gas reactions to store large amounts of thermal energy with minimal loss during the storage period [1–3]. Salt hydrates deserve particular attention due to the possibility of using collector-grade heat for the dehydration process and releasing heat through hydration at a later stage [4–6]. Reviews of TCES developments note that the transition from potentially effective chemistry to an efficient piece of equipment involves several interacting criteria such as bed stability, access to gas, heat transfer path length, pressure loss, reactor geometry, and system integration [7,8]. Consequently, the choice of suitable materials is far from being sufficient for a viable design of a TCES system.

These challenges become particularly pronounced in the case of open TCES reactors, whose hardware is relatively simple, but the performance strongly depends on parameters like air mass flow rate, bed thickness, reactor channel configuration, and inlet temperature [9–11]. Increased air flow that is beneficial for the enhancement of conversion degree might have a detrimental effect on collector performance, or reduce temperature lift at the expense of increased fan power consumption. A thicker reactor bed increases its reagent content, but reduces the effectiveness of operation at the rear of the bed. An elongated bed can

improve the storage degree until nonuniformity of reactions and thermal losses offset its contribution to performance. Therefore, TCES research has started focusing not only on materials, but on reactors and system integration [12,13].

The PV/T-TCES combination adds yet another layer of complexity. A photovoltaic-thermal collector can supply electricity while preheating the air stream for the TCES charging loop. Hybrid studies involving collectors and sorption storage units demonstrate the advantage of considering collector performance and electricity production jointly rather than independently [14–16]. This consideration is essential in the case of PV/T-TCES charging since changes in a certain parameter such as air mass flow rate might affect not only the performance of the reactor, but also the operation of the PV/T system and collector outlet temperature. Heat recovery in the cross flow heat exchanger can affect the balance of PV/T electricity against grid electricity needed to supply auxiliary heaters and fans.

Consequently, PV/T-TCES designs can be analyzed not only in terms of conversion degree, stored heat, and efficiency, but also in terms of electricity consumption and renewable electricity fraction. Different designs can be compared on different criteria, and multi-criteria ranking of alternatives requires that the criteria, their weights, and physical meanings are identified explicitly [17]. In the context of PV/T-assisted charging, what matters is whether the PV/T-TCES design can produce high-quality storage while relying minimally on external electricity. The research question in the current study reflects this perspective: *Which system architecture, air mass flow rate, and bed dimensions allow the highest-quality charging in an open PV/T-TCES unit with heat recovery?*

In this regard, the paper proposes to study four aspects of the current problem: PV/T-TCES architecture, air mass flow rate, bed thickness, and bed length. The evaluation will be based on the Electricity-Aware Charging Quality Index (EACQI) that includes traditional performance metrics plus an additional metric representing the storage-to-external-electricity ratio. Design guidelines will differentiate between balanced operation, storage-led operation, efficiency-led operation, and grid-sparing operation to answer the charging design question posed in the introduction.

Figure 1. Integrated charging loop.

2. System and Charging-Decision Case Matrix

2.1. PV/T-TCES-HEX charging loop

The considered charging system includes an open air flow in which air initially enters the heat exchanger, after passing through the air PV/T collector gets further heating from the auxiliary heater, and goes into the packed reactor equipped with a multilayered bed based on $CaCl_2$. Reactor exhaust gases return via the heat exchanger in order to reclaim part of sensible heat prior to air discharge. The PV/T collector provides thermal and electric energies to the system, and the auxiliary heater ensures that the reactor inlet air attains the

desired temperature. Such a system is contrasted with a TCES-HEX system without PV/T module and a TCES system without both modules PV/T and heat recovery.

Figure 1 depicts the charging loop consisting of the heat-exchange unit, the PV/T module, the auxiliary heater, and the packed-bed reactor; reactor exhaust is shown returning back into the inlet air to recover part of sensible heat prior to the final discharge. This physical picture defines the four levels at which charging decisions can be made: system architecture, air flow rate, bed thickness, and bed length.

From the hardware viewpoint, the decision-making problem involves a chain of energy conversion operations, not independent variables. In particular, the PV/T module alters both the input heat and electric energy available for system functioning, whereas the heat exchange affects the temperature rise demanded from the auxiliary heater. That is why the following comparison starts with the system architecture.

2.2. Variables for evaluation

There are seven evaluation criteria included in the charging decision matrix. There are six variables associated with every modeled charging scenario, and these are: conversion extent X, energy in storage Q_s, PV/T energy input $W_{PV/T}$, external electrical energy use W_e, power assurance rate PAR, and overall efficiency η. The seventh variable to be evaluated is the storage performance index, P_s which is defined as:

$$P_s = \frac{Q_s}{W_e}. \tag{1}$$

This parameter is selected since even with high energy content for the charging cycle, it would not necessarily result to being a good choice if it needs substantial amount of purchased electrical energy. On the other hand, P_s reflects the extent of efficiency of the system in converting the electricity from sources not derived from the PV/T into thermal storage energy.

These parameters are divided into benefit-type and cost-type reactions. Benefit type parameters include conversion degree, energy storage, PV/T contribution, power assurance ratio, thermal efficiency, and storage productivity. External electricity consumption is considered a cost type parameter. Given the benefit-type parameter, the normalized performance score of alternative j with respect to criterion i is

$$S_{ij}^{+} = \frac{x_{ij} - x_i^{\min}}{x_i^{\max} - x_i^{\min}}, \tag{2}$$

whereas the normalized score for external electricity is

$$S_{ij}^{-} = \frac{x_i^{\max} - x_{ij}}{x_i^{\max} - x_i^{\min}}. \tag{3}$$

Both Eqs. (2) and (3) allow placing all criteria within the same 0 to 1 range. The larger the normalized value, the better the corresponding result. It is required due to the fact that initial values for different criteria represent numbers with distinct units of measure and opposite preferences. Otherwise, energy stored and electricity consumed cannot be compared.

The value of the Electricity Aware Quality Index of Charging is determined as

$$\mathrm{EACQI}_j = \sum_{i=1}^{n} w_i S_{ij}, \qquad \sum_{i=1}^{n} w_i = 1, \tag{4}$$

where S_{ij} denotes either S_{ij}^{+} or S_{ij}^{-} depending on the criterion type. The balanced weights for design-variable cases are

$$\{w_X, w_{Q_s}, w_{W_{PV/T}}, w_{W_e}, w_{PAR}, w_\eta, w_{P_s}\} = \{0.05, 0.25, 0.10, 0.20, 0.05, 0.20, 0.15\}. \tag{5}$$

These weights give priority to stored heat, electricity, conversion efficiency, and storage productivity. The conversion rate and power assurance rate are kept, since they signal reaction completion and PV/T assistance; however, they can not overpower the ranking because the answer to the central question should be good charging design, not necessarily high conversion design. For the architecture comparison, there are only three relevant criteria: PV/T energy, electricity, and thermal efficiency; the architecture score normalizes the weights accordingly.

The hierarchy of the criteria used and the corresponding levels applied are summarized in Table 1. The panel illustrates the seven parameters required for the evaluation of EACQI together with the architecture, flow rate, thickness, and length levels needed to create the charging-case matrix (Figure 2).

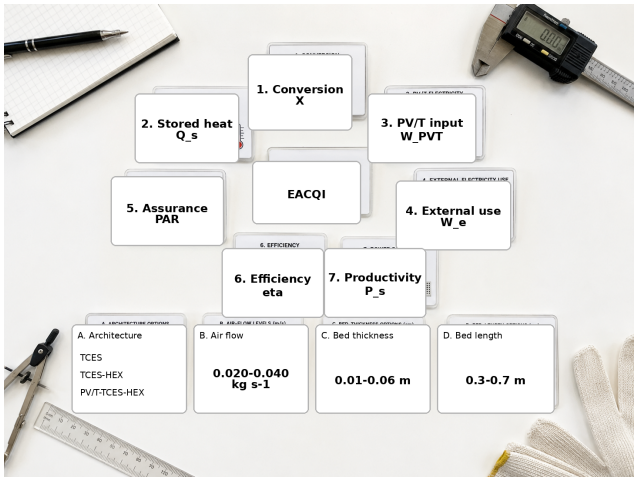

Figure 2. EACQI case matrix.

It needs to be emphasized in the method panel that EACQI does not add a new measurable attribute to the reactor. It is an explicit numerical evaluation score obtained using the measured or calculated charging properties of the system. The only change of preference is observed in cost treatment of W_e.

Table 1. EACQI criteria.

Criterion	Direction	Role in electricity-aware charging selection
Conversion degree, X	Benefit	Confirms reaction progress but is not treated as the only design target.
Storage energy, Q_s	Benefit	Measures useful thermal energy charged into the thermochemical bed.
PV/T contribution, $W_{PV/T}$	Benefit	Indicates renewable thermal/electrical participation in the charging loop.
External electricity, W_e	Cost	Penalizes reliance on grid or non-PV/T auxiliary electricity.
Power-assurance rate, PAR	Benefit	Measures the degree to which PV/T electricity supports equipment demand.
Thermal efficiency, η	Benefit	Captures overall charging quality after losses and auxiliary inputs.
Storage productivity, P_s	Benefit	Relates stored heat to external electricity requirement.

These criteria do not allow the results to be interpreted in a narrow-minded manner. For instance, the first criterion in Table 1, where only one maximum of X, Q_s, and η is achieved, is not sufficient for design evaluation. The solution must be further analyzed to see whether it increases the effectiveness of energy storage and does not impose too much electricity consumption penalty on the system. Such approach is reasonable for hybrid PV-T/TCES systems, because both PV/T and heat recovery branches bring value if they decrease the auxiliary cost of charging.

3. Results and Discussion

3.1. Architecture-level ranking

The architecture comparison is probably the strongest system-level result of the work. The combined PV/T-TCES-HEX system is the most thermally efficient one among the three compared configurations with the lowest external electricity consumption. Compared to the standalone TCES option, the PV/T-TCES-HEX system decreases external electricity consumption from 29.26 to 11.86 kWh that is equal to 59.47%, while increasing total thermal efficiency from 22.69% to 56.00%.

Based on the rankings of the architectures seen in Table 2, the PV/T architecture option is clearly more than just a minor improvement. In effect, it changes the nature of the architecture from one where all work is based on energy recovery, to one involving renewables in the energy supply and management process. The heat exchanger itself already provides an efficiency gain and reduced electricity demand, but the PV/T-TCES-HEX architecture is the only architecture configuration that improves thermal efficiency while also providing additional renewable energy input and reduced external electricity. That is why the architectural choice is more important than any geometry modification made within it.

Table 2. Architecture ranking.

Architecture	$W_{PV/T}$ (kWh)	W_e (kWh)	η (%)	W_e reduction (%)	EACQI	Rank
PV/T-TCES-HEX	3.83	11.86	56.00	59.47	1.000	1
TCES-HEX	0.00	15.86	41.85	45.80	0.538	2
TCES-only	0.00	29.26	22.69	0.00	0.000	3

Figure 3 visually illustrates how the physical additions involved in different architecture configurations are different. The TCES-only configuration includes the reactor and charging system, while the TCES-HEX architecture configuration includes exhaust heat recovery. Lastly, the PV/T-TCES-HEX configuration includes both the above mentioned hardware systems plus renewables in the form of electricity and solar power. In other words, the best-performing architecture is not a product of changing any reactor geometric parameter, but rather a result of adding two energy management units that reduce external energy necessary for charging the same type of storage bed.

Figure 3. Hardware comparison among different architectures.

3.2. Air mass flow rate

The results of air-flow address the operational aspect of the research question. While 0.025 kg s^{-1} yields maximum EACQI values for balanced operation, the adjacent flows of 0.020 and 0.030 kg s^{-1} should also be regarded as significant from an operational standpoint.

Of these, the former yields maximum storage capacity due to the least consumption of electrical power from the outside. The latter yields maximum energy in the storage among these three options, along with maximum energy conversion.

The numbers in Table 3 make the physical trade-off very clear. While higher air mass flow (0.020 to 0.040 kg s^{-1}) results in an increase in conversion from 79.48% to 99.99%, it causes external electricity consumption to increase from 6.96 to 17.06 kWh and thermal efficiency to drop from 80.02% to 40.15%. Hence, the reason for rejecting the highest air flow rate case as an optimal operating point despite having almost total conversion becomes evident. In view of this observation, the practical charging approach cannot treat conversion degree as the primary objective.

Table 3. Air-flow ranking.

$\dot{m}_{air}$ (kg s^{-1})	X (%)	Q_s (kWh)	$W_{PV/T}$ (kWh)	W_e (kWh)	η (%)	P_s	EACQI	Rank
0.020	79.48	5.57	3.32	6.96	80.02	0.800	0.600	2
0.025	91.64	6.24	3.58	9.40	66.38	0.664	0.601	1
0.030	99.01	6.64	3.83	11.86	56.00	0.560	0.572	3
0.035	99.73	6.81	4.03	14.42	47.23	0.472	0.490	4
0.040	99.99	6.85	4.25	17.06	40.15	0.402	0.400	5

The air-flow configurations depicted in Figure 4 are shown separately in order to highlight the operating compromise. The 0.025 kg s^{-1} is kept as the balanced case, as it falls in between the electricity-saving 0.020 kg s^{-1} case and the energy-storage dominated 0.030 kg s^{-1} case. Although the latter two flows have the capability to achieve high conversion ratios, their electricity cost increases much faster than their benefits from charging. From the practical standpoint, the figure and the table above can be used to argue in favor of a 0.020–0.030 kg s^{-1} operational range.

Figure 4. Air-flow cases.

3.3. Bed thickness

The bed thickness sequence is the split point between maximizing heat storage and balancing charge quality improvement. While the largest bed (0.05 m thick) contains the most heat, the optimal EACQI can be obtained using the smallest one (0.04 m), since it provides full conversion, retains strong thermodynamic efficiency, and prevents electricity penalty associated with the larger size. Too thin beds can convert easily but do not possess sufficient amount of reactive inventory; conversely, too large beds store a lot of heat while being inefficient in terms of electricity awareness.

The numbers presented in Table 4 justify two statements that can be drawn for the design of such a project. The first one claims that the optimal thickness is 0.04 m. In contrast with some criteria which maximize certain variable values, this statement claims a design

which does not have a severe flaw in its characteristics. Another claim that can be made here is that 0.05 m bed is still useful when the project is based on storing as much heat as possible. This is a significant remark that should be highlighted since, obviously, a storage-oriented project and an electricity-limited project should not utilize the same bed thickness.

Table 4. Thickness ranking.

Thickness (m)	X (%)	Q_s (kWh)	$W_{PV/T}$ (kWh)	W_e (kWh)	η (%)	P_s	EACQI	Rank
0.01	100.00	1.71	1.23	5.09	33.66	0.336	0.250	6
0.02	100.00	3.03	2.33	6.53	46.39	0.464	0.542	4
0.03	100.00	4.26	3.11	7.88	54.09	0.541	0.714	3
0.04	100.00	5.50	3.61	9.55	57.55	0.576	0.802	1
0.05	99.00	6.64	3.83	11.86	56.00	0.560	0.755	2
0.06	35.00	4.61	3.29	11.01	41.85	0.419	0.393	5

The modules of bed thickness in Figure 5 represent the ranking of the rows in terms of geometric representation. By adding more packed material, there would be an increase in reactive material but this will affect the ability to make use of the downstream material with respect to the charging stream. In the case of the 0.04 m module, there is sufficient storage capacity and is completely utilized in the ranking while the 0.05 m module has greater storage capacity than utilization.

Figure 5. Modules of Bed Thickness.

3.4. Bed length

There is no monotonic design response regarding the reactor bed length. Shorter beds have a higher degree of conversion, although they do not produce the best result for the charging process. The reactor with the bed length of 0.5 m stores the maximum amount of heat energy, produces the greatest output from the PV/T system, and demonstrates the highest efficiency. Hence, this design is ranked number one based on the results of the EACQI calculation.

These numbers help explain why the degree of conversion is a bad design parameter. The shortest bed length (0.3 m) yields 99.00% conversion rate, but stores 5.31 kWh of heat energy, making it the worst design choice. On the contrary, the 0.5 m bed is inferior to it in terms of degree of conversion at 80.00% but provides 7.07 kWh of heat energy and 58.73% of efficiency (Table 5).

It can be understood from Figure 6 that longer hardware provides more capacity until a certain limit, after which no further enhancement of the charging space is obtained. Thus, the optimal length of 0.5 m can be seen to be a kind of a limiting factor in terms of reachability rather than being merely the biggest reactor.

Table 5. Length ranking.

Length (m)	X (%)	Q_s (kWh)	$W_{PV/T}$ (kWh)	W_e (kWh)	η (%)	P_s	EACQI	Rank
0.3	99.00	5.31	3.62	11.30	46.96	0.470	0.250	5
0.4	97.00	6.64	3.84	11.86	56.00	0.560	0.689	2
0.5	80.00	7.07	3.88	12.04	58.73	0.587	0.766	1
0.6	48.00	6.53	3.74	11.79	54.31	0.554	0.569	3
0.7	49.00	5.83	3.71	11.49	50.68	0.507	0.404	4

Figure 6. Length modules of the beds.

3.5. Priority robustness

This ranking can be useful for a practical design but other priorities such as higher storage capability, higher efficiency, or increased grid independence might be desirable. Thus, the same normalized case matrix was considered with four priority scenarios: balanced, storage-led, efficiency-led, and grid-sparing. The system design still uses PV/T-TCES-HEX since it clearly outperforms other architectures from the architecture-level comparison. However, there are different air flow and packed bed thicknesses while the optimal bed length equals to 0.5 m.

The recommendations from Table 6 give an opportunity to implement the proposed design approach into practice. To achieve a balanced system design it is necessary to consider 0.025 kg s^{-1}, 0.04 m thickness, and 0.5 m length. In case of higher priorities on storing energy, the system needs to increase air flow to 0.030 kg s^{-1} and thickness to 0.05 m. In case of efficiency-led and grid-sparing approaches, it needs to switch the flow rate to 0.020 kg s^{-1} maintaining thickness and length parameters at 0.04 m and 0.5 m correspondingly. These alternatives also keep the PV/T-TCES-HEX system design.

Table 6. Priority-based recommendations.

Priority setting	Air flow (kg s^{-1})	Thickness (m)	Length (m)
balanced	0.025	0.04	0.5
storage-led	0.030	0.05	0.5
efficiency-led	0.020	0.04	0.5
grid-sparing	0.020	0.04	0.5

As for the priority configuration in Figure 7, the storage-led case is characterized by the ability to carry a higher charging load in return for additional stored energy. Efficiency-led and grid-sparing cases tend to reduce the air flow and maintain bed thickness at 0.04 m. Both priority-based approaches use the length equal to 0.5 m, which gives more robustness to length than flow-rate results.

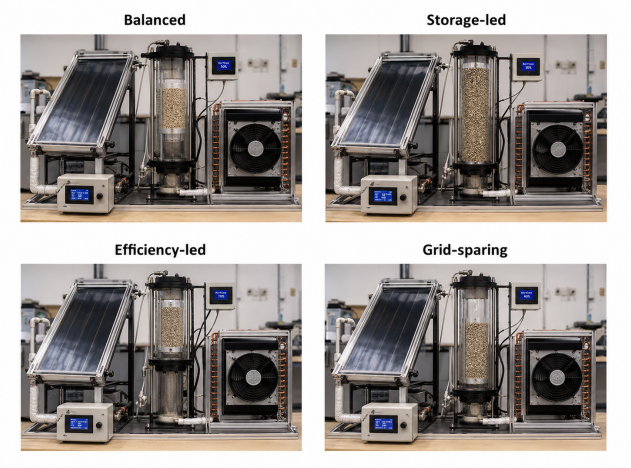

Figure 7. Priority-based designs.

The last design illustration shown in Figure 8 represents the answer in terms of illustrations that is given to the research question through this article. In accordance with the preferences of a balanced system, the optimal design is the integrated design consisting of PV/T-TCES-HEX modules in which the flow rate would be 0.025 kg s^{-1}, the thickness of the packed-bed would be 0.04 m, and the reactor length would be 0.5 m. For other designs, the reactor architecture and length remain the same, but the parameters vary depending on the goals.

Figure 8. Recommended design configuration.

4. Conclusions

What architecture, air-flow state, and reactor dimensions yield the most electricity-aware charging quality in an open PV/T-aided TCES with exhaust heat recovery? This question has yielded a precise answer. On the architectural level, the optimal design configuration is PV/T-TCES-HEX, which saves 59.47% of externally supplied electricity compared to the TCES alone operation and increases thermal efficiency to 56.00%. Thus, the PV/T panel and HEX become enablers of the optimal charging design rather than optional parts of it.

On the operational level, the balanced air mass flow rate is 0.025 kg s^{-1}, yet the physically sensible design choice is the 0.020–0.030 kg s^{-1} air flow range, where the lower limit is preferable if the emphasis is on minimizing electricity load or maximizing efficiency, while the upper limit is better if storage energy or completeness of conversion is the priority.

This result proves that air mass flow should be regarded as an adjustable control parameter rather than as the optimum.

Regarding the reactor geometry, 0.04 m is the best balanced reactor thickness since it ensures complete conversion, maximum efficiency, and the moderate electricity load. An increase to 0.05 m can be considered only if the capacity of the storage is a priority over other considerations. As for bed length, 0.5 m turns out to be the most universal among the tested lengths due to the fact that although shorter reactors demonstrate higher conversion degree, the 0.5 m-long reactor provides the best performance compromise between storage and efficiency.

In conclusion, we find that optimal design results from the right integration of system elements into the reactor geometry: PV/T panel and HEX decrease the electrical cost, whereas the intermediate dimensions ensure good storage potential without excessive transport burden. The recommended design is the balanced PV/T-TCES-HEX charging system with 0.025 kg s^{-1} air flow, 0.04 m thick bed, and 0.5 m long reactor. If, however, a design optimization based on storage priority is required, the PV/T-TCES-HEX system with 0.030 kg s^{-1} and 0.05 m bed thickness can be applied, whereas if one wishes to minimize the electricity cost or maximize efficiency, then 0.020 kg s^{-1} air flow rate will be better. These guidelines are consistent with the goals of this paper.

The boundary of numerical investigation of the problem is the tested matrix of charge cases and the transparent method of ranking according to the weighted index. The proposed region should be validated in transient weather and humidity, partial day solar charging, and experimental fan-heater performance maps. Within the scope of investigated operational parameters, electricity awareness reveals new design options that conversion-only and storage-only approaches fail to reveal.

References

[1] Aydin, D., Casey, S. P., & Riffat, S. (2015). The latest advancements on thermochemical heat storage systems. Renewable and Sustainable Energy Reviews, 41, 356-367.

[2] Abedin, A. H., & Rosen, M. A. (2011). A critical review of thermochemical energy storage systems. The open renewable energy journal, 4(1), 42-46.

[3] Spietz, T.; Fryza, R.; Lasek, J.; Zuwala, J. Thermochemical Energy Storage Based on Salt Hydrates: A Comprehensive Review. *Energies* **2025**, *18*, 2643.

[4] N'Tsoukpoe, K. E., Schmidt, T., Rammelberg, H. U., Watts, B. A., & Ruck, W. K. (2014). A systematic multi-step screening of numerous salt hydrates for low temperature thermochemical energy storage. Applied Energy, 124, 1-16.

[5] Lin, J., Zhao, Q., Huang, H., Mao, H., Liu, Y., & Xiao, Y. (2021). Applications of low-temperature thermochemical energy storage systems for salt hydrates based on material classification: A review. Solar Energy, 214, 149-178.

[6] Liu, X.; Li, X.; Wang, Z.; Zhang, Y. A systematic evaluation of thermochemical heat storage based on hydration/dehydration of salt hydrates for heating applications. *Renewable Energy* **2025**, *245*, 122831.

[7] Aarts, J.; Fischer, H.; Adan, O.; Huinink, H. Towards stable performance of salt hydrates in thermochemical energy storage: A review. *Journal of Energy Storage* **2025**, *114*, 115726.

[8] Moulakhnif, K.; Ait Ousaleh, H.; Sair, S.; Bouhaj, Y.; El Majd, A.; Ghazoui, M.; Faik, A.; El Bouari, A. Renewable approaches to building heat: exploring cutting-edge innovations in thermochemical energy storage for building heating. *Energy and Buildings* **2024**, *318*, 114421.

[9] Michel, B., Mazet, N., & Neveu, P. (2014). Experimental investigation of an innovative thermochemical process operating with a hydrate salt and moist air for thermal storage of solar energy: Global performance. Applied Energy, 129, 177-186.

[10] Mukherjee, A., Pujari, A. S., Shinde, S. N., Kashyap, U., Kumar, L., Subramaniam, C., & Saha, S. K. (2022). Performance assessment of open thermochemical energy storage system for seasonal space heating in highly humid environment. Renewable Energy, 201, 204-223.

[11] Abedin, A. H., & Rosen, M. A. (2012). Closed and open thermochemical energy storage: Energy-and exergy-based comparisons. Energy, 41(1), 83-92.

[12] Zhao, Q., Lin, J., Huang, H., Wu, Q., Shen, Y., & Xiao, Y. (2021). Optimization of thermochemical energy storage systems based on hydrated salts: A review. Energy and Buildings, 244, 111035.

[13] John, M. K.; Vishnu, K.; Vishnu, C.; Bandaru, R.; Muraleedharan, C. Experimental and numerical investigations on an open thermochemical energy storage system using low-temperature hydrate salt. *Thermal Science and Engineering Progress* **2024**, *53*, 102749.

[14] Guo, C., Ji, J., Sun, W., Ma, J., He, W., & Wang, Y. (2015). Numerical simulation and experimental validation of tri-functional photovoltaic/thermal solar collector. Energy, 87, 470-480.

[15] Thinsurat, K.; Bao, H.; Ma, Z.; Roskilly, A. P. Performance study of solar photovoltaic-thermal collector for domestic hot water use and thermochemical sorption seasonal storage. *Energy Conversion and Management* **2019**, *180*, 1068–1084.

[16] Jiang, L.; Wang, R. Z.; Roskilly, A. P.; Wang, L. W. Thermodynamic analysis of a hybrid sorption thermal energy storage system combined with photovoltaic-thermal collectors. *Energy Conversion and Management* **2022**, *268*, 115993.

[17] Al-Abri, Z. M.; Alawasa, K. M.; Al-Abri, R. S.; Al-Hinai, A. S.; Awad, A. S. A. Multi-Criteria Decision-Making Approach for Optimal Energy Storage System Selection and Applications in Oman. *Energies* **2024**, *17*, 5197.